The Response of the Zonally Averaged Circulation to Stratospheric Ozone Reductions

MARK R. SCHOEBERL AND DARRELL F. STROBEL

Naval Research Laboratory, Washington, D.C. 20375

(Manuscript received 23 November 1977, in final form 10 May 1978)

ABSTRACT

The effects of various ozone density reductions on the zonally averaged circulation are evaluated with a numerical quasi-geostrophic model. If the ozone perturbations are confined to the polar regions and are minuscule on a global basis as was characteristic of the August 1972 solar proton event, then our calculation indicate a negligible effect on the mean circulation. For global ozone perturbations by predicted halocarbon pollution, we calculate about a 10% reduction in the zonal jet strength and less than a 5% change in global mean stratospheric temperature. Large, uniform ozone reductions (>50%) produce significant effects on the mean circulation: a substantial collapse of the stratosphere due to cooler temperatures, and a weak polar night jet. The reflection and transmission of quasi-stationary planetary waves in the middle atmosphere are computed to be insensitive to solar activity as extreme as the August 1972 solar proton event. It thus seems improbable that planetary waves are a viable mechanism for solar-weather interactions that involve perturbations of the zonally averaged circulation by ozone density reductions.

1. Introduction

Considerable effort has been expended to assess the impact of chemical pollutants on the stratospheric environment. These pollutants catalytically attack ozone, the principal atmospheric absorber of biologically harmful solar UV radiation. This UV radiation also heats the stratosphere and drives the zonally averaged (mean) circulation of the middle atmosphere. Since the stratosphere is a relatively stagnant region of the atmosphere, environmental assessment of pollution effects will depend critically on the response of stratospheric dynamics to the changes in radiative forcing that accompany pollution induced ozone reductions.

Our recently developed numerical model (Schoeberl and Strobel, 1978; hereafter referred to as I) has been used to compute the response of the mean circulation to ozone density perturbations in the middle atmosphere. We have designed a series of numerical experiments to simulate observed natural perturbations and predicted man-made perturbations. Both the immediate time-dependent response and the final asymptotic state (steady-state solution) for these perturbations have been examined

2. Model

In I we previously studied the zonally averaged circulation of the middle atmosphere (15–125 km) with a quasi-geostrophic, numerical model that explicitly includes a self-consistent calculation of solar radiative heating due to O_2 and O_3 absorption, Newtonian cooling, Rayleigh friction and tropopause boundary conditions based on climatological averages. In order to calculate the effects of ozone reduction we must also compute the globally averaged atmospheric fields, denoted by angle braces, as well as the zonally averaged fields, denoted by an overbar, which are equal to the difference between zonally averaged variables and globally averaged variables.

The globally averaged atmosphere is assumed to be motionless, hydrostatic and in approximate radiative balance. With the vertical coordinate $z=\ln(p_0/p)$, where p_0 is a reference pressure taken to be 100 mb, the governing equations of the globally averaged atmosphere are

$$\frac{\partial\langle T\rangle}{\partial t}=\langle H\rangle-\langle\alpha\rangle\langle T\rangle-\langle b\rangle, \tag{1}$$

$$\frac{\partial\langle\phi\rangle}{\partial z}=R\langle T\rangle, \tag{2}$$

where α is the Newtonian cooling coefficient, b the mean cooling rate, H the heating rate per unit mass, T temperature, ϕ geopotential height and R the dry air gas constant.

The zonally averaged circulation is governed by

$$\left(\frac{\partial}{\partial t}+k_r\right)\left\{\frac{1}{\cos\theta}\frac{\partial}{\partial\theta}\left[\left(\frac{\cos\theta}{\gamma^2+\sin^2\theta}\right)\frac{\partial\bar{\phi}}{\partial\theta}\right]\right\}+(2\Omega a)^2e^z$$
$$\times\frac{\partial}{\partial z}\left[\frac{e^{-z}}{S}\left(\frac{\partial}{\partial t}+\langle\alpha\rangle\right)\frac{\partial\bar{\phi}}{\partial z}\right]=e^z\frac{\partial}{\partial z}\left(\frac{e^{-z}(2\Omega a)^2\bar{H}}{S}\right), \tag{3}$$

TABLE 1. A summary of O_3 reductions experiments.

O_3 reduction (%)	Solar flux	Max $\bar{u}$ ($m\ s^{-1}$)	Height (km)	$\langle T \rangle$	Height (km)	Summer polar stratopause $\langle T \rangle + \bar{T}(K)$	Height (km)	Winter polar mesopause $\langle T \rangle + \bar{T}(K)$	Height (km)	Max $\bar{v}$ ($m\ s^{-1}$) (below 80 km)	Height (km)	Max $\bar{w}^*$ ($cm\ s^{-1}$)	Height (km)	Amplitude $m=1$ (50 km, 50°N)	Phase (°W) $m=1$ (50 km, 50°N)	Amplitude $m=2$ (50 km, 50°N)	Phase (°W) $m=2$ (50 km, 50°N)
00	1.0×	86	64	271	47.0	317	51.0	169	98.0	2.06	73.0	−0.703	83.0	497 gpm	−44	179 gpm	93
25	1.0×	75	61	263	44.0	304	47.0	163	96.0	1.75	72.0	−0.612	82.0	429	−43	185	103
50	1.0×	64	59	257	40.0	292	43.0	156	92.0	1.42	71.0	−0.51	80.0	364	−48	162	114
75	1.0×	58	52	249	39.0	286	40.0	143	89.0	1.14	66.0	−0.415	78.0	321	−59	152	119
Halocarbon	1.0×	78	63	263	51.0	306	50.0	169	97.0	1.85	72.0	−0.651	83.0	420	−43	178	127
00	1.2×	101	65	283	48.0	336	52.0	181	101.0	2.43	71.0	−0.8	85.0	598	−48	171	81
00	1.1×	94	65	277	47.6	327	51.0	175	99.0	2.25	71.5	−0.75	84.0	551	−45	177	87
00	0.9×	79	63	265	47.0	307	50.0	164	97.0	1.87	71.0	−0.65	82.0	441	−43	176	100
00	0.8×	72	60	259	46.5	297	50.0	158	95.0	1.68	69.0	−0.593	81.0	387	−44	168	107

* $\bar{w} \times (7 \times 10^5$ cm).

where k_r is the Rayleigh friction coefficient, $\gamma = k_r/2\Omega$, where Ω is the earth's rotational frequency, a is the earth's radius, S the static stability and θ latitude. The mean zonal wind is given by

$$\bar{u} = \frac{-\sin\theta}{2\Omega a(\gamma^2 + \sin^2\theta)} \frac{\partial \bar{\phi}}{\partial \theta}. \tag{4}$$

The Newtonian cooling coefficient $\langle \alpha \rangle$ is based on Dickinson's (1973) detailed IR calculations and is assumed invariant on pressure surfaces. Since the globally averaged temperature profile is fairly well known (CIRA, 1972) and the major contributions to solar heating, $\langle H \rangle$, can be accurately and self-consistently computed as described in I, $\langle b \rangle$ is chosen to obtain radiative balance for the CIRA (1972) $\langle T \rangle$ profile when $\partial \langle T \rangle / \partial t = 0$ in Eq. (1). Below 70 km our derived $\langle b \rangle$ values are in accord with the Dickinson (1973) results. These $\langle b \rangle$ values are also assumed invariant (with time and changes in atmospheric structure) on pressure surfaces in all calculations. The boundary conditions used for the numerical solution of Eq. (3) are given in I. For small O_3 density perturbations, it is a reasonable assumption that the IR radiative transfer and hence cooling rates will not be seriously altered. But for large O_3 density perturbations our computations should be regarded as only qualitatively correct. The photochemical acceleration of the thermal relaxation rate was neglected in Eqs. (1) and (3) because the O_3 densities were specified; the catalytic reactions have a weak temperature dependence, and the rate depends on the nature of the chemical perturbation (pollutant). The neglect of this rate will only affect the time dependent response of the stratopause region.

3. Uniform ozone density reductions

Probably the simplest experiment which can be performed is to uniformly reduce ozone everywhere. Three such experiments were performed with a 25, 50 and 75% ozone reduction, respectively. Selected asymptotic values of the meteorological variables are presented in Table 1 as diagnostic indicators of the mean circulation.

With any uniform O_3 reduction two important effects occur: first, the globally averaged stratospheric temperature decreases which causes pressure surfaces to descend in altitude; second, the differential heating rate that drives the mean circulation decreases which leads to a smaller meridional temperature gradient and a weaker polar night jet.

These effects are quantitatively displayed in Figs. 1 and 2 where the globally averaged heating and temperature profiles, respectively, are presented. The pole-to-pole differential heating rate is proportional to the globally averaged heating rate $\langle H \rangle$. We note in Fig. 2 that the stratopause and mesopause descend significantly as O_3 density reductions increase. Also, radiation

in the Hartley and Huggins bands penetrates deeper and heats a denser region of the atmosphere. At unit optical depth the peak heating rate per unit mass is smaller, as illustrated in Fig. 1. The globally averaged temperature profiles clearly reflect this effect in Fig. 2. A lower mesosphere results from the smaller vertical extent of a cooler stratosphere.

Fig. 3 shows the structure of the polar night jet for each of the three experiments along with the unperturbed atmosphere. Note that the height coordinates, which represent the globally averaged height of individual pressure surfaces, are different for each figure as a consequence of the altitude variation of pressure surfaces.

Ozone reduction leads to not only a cooler, collapsing stratosphere, but by the thermal wind relation, to descending zonal jets which decrease in intensity as seen in Fig. 3. Note that as the jets weaken the influence of tropospheric height fields extends slightly higher into the stratosphere. This is especially apparent in the summer hemisphere.

From steady-state calculations the stratospheric response time to perturbations cannot be inferred, although the damping rates k_r and $\langle\alpha\rangle$ would be expected to yield a characteristic relaxation time. A time-dependent calculation with a 75% O_3 density reduction switched on at $t=0$ is illustrated by the changes in $\bar{u}$ at 62.5°N and $\bar{T}$ at 87.5°N (winter hemisphere) at various constant altitudes in Fig. 4. The *e*-folding rate for the zonal wind (Fig. 4a) is ~5 days in the mesosphere and upper stratosphere and somewhat longer in the middle stratosphere. The temperature perturbations in Fig. 4b are more complicated as a result of the collapsing stratosphere. For example, at 95 km the temperature initially decreases from the reduced heating but eventually increases as the warm thermosphere descends to lower levels. Similarly the warm winter mesosphere descends and negates a large temperature decrease in

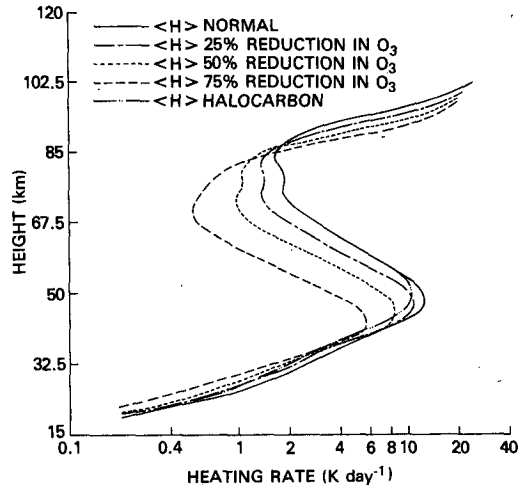

FIG. 1. The globally averaged heating rate (K day^{-1}).

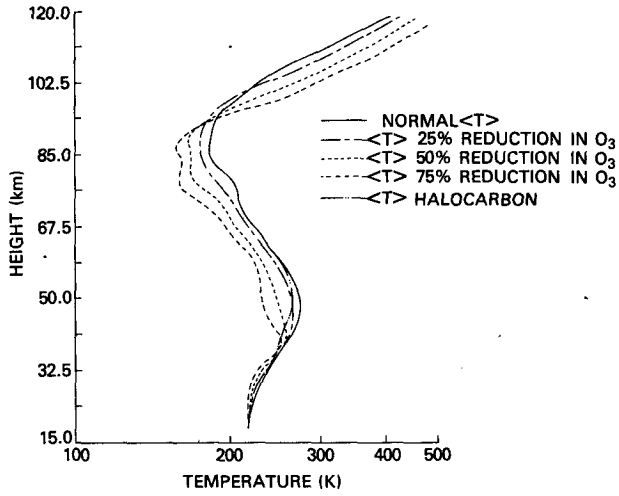

FIG. 2. The globally averaged temperature (K).

the vicinity of the stratopause at 55 km. At this altitude a relaxation time of ~5 days could be deduced, although admittedly the interference of time constants from Fig. 4b is not straightforward. Another interesting feature of Fig. 4 is the slight increase in $\bar{u}$ and $\bar{T}$ after 15 days. This oscillation in the response is a result of the interaction of the globally averaged temperature with the zonal mean perturbations through the static stability S. As $\langle T\rangle$ decreases, S also decreases and the zonally averaged temperature approaches radiative equilibrium. As shown in I, the polar night jets are much stronger for a radiative equilibrium atmosphere. Thus this effect tends to counteract the decrease in the meridional heating gradient which weakens the pole-to-pole circulation.

4. Realistic ozone reductions

The results of the previous computer experiments cannot be realistically applied to the stratosphere since the column O_3 density reductions are substantially larger than both observed and predicted perturbations of the ozone layer [Heath *et al.*, 1977; Committee on Impact on Stratospheric Change (CISC), 1976]. They do, however, serve as benchmarks to evaluate pollution effects. To provide a realistic assessment of the potential impact on stratospheric dynamics two additional computer experiments were performed. Heath *et al.* (1977) observed ozone reductions during the August 1972 solar proton event. A maximum O_3 density reduction of ~22% was observed at 44 km and confined to polar regions. A suitable model based on their data was constructed.

A time-dependent simulation of the dynamical response of the middle atmosphere to the solar proton event showed negligible impact. The strength of the polar night jet remained constant (<1% change) and the globally averaged stratospheric temperature changed by less than 1 K at 45 km. In the polar regions

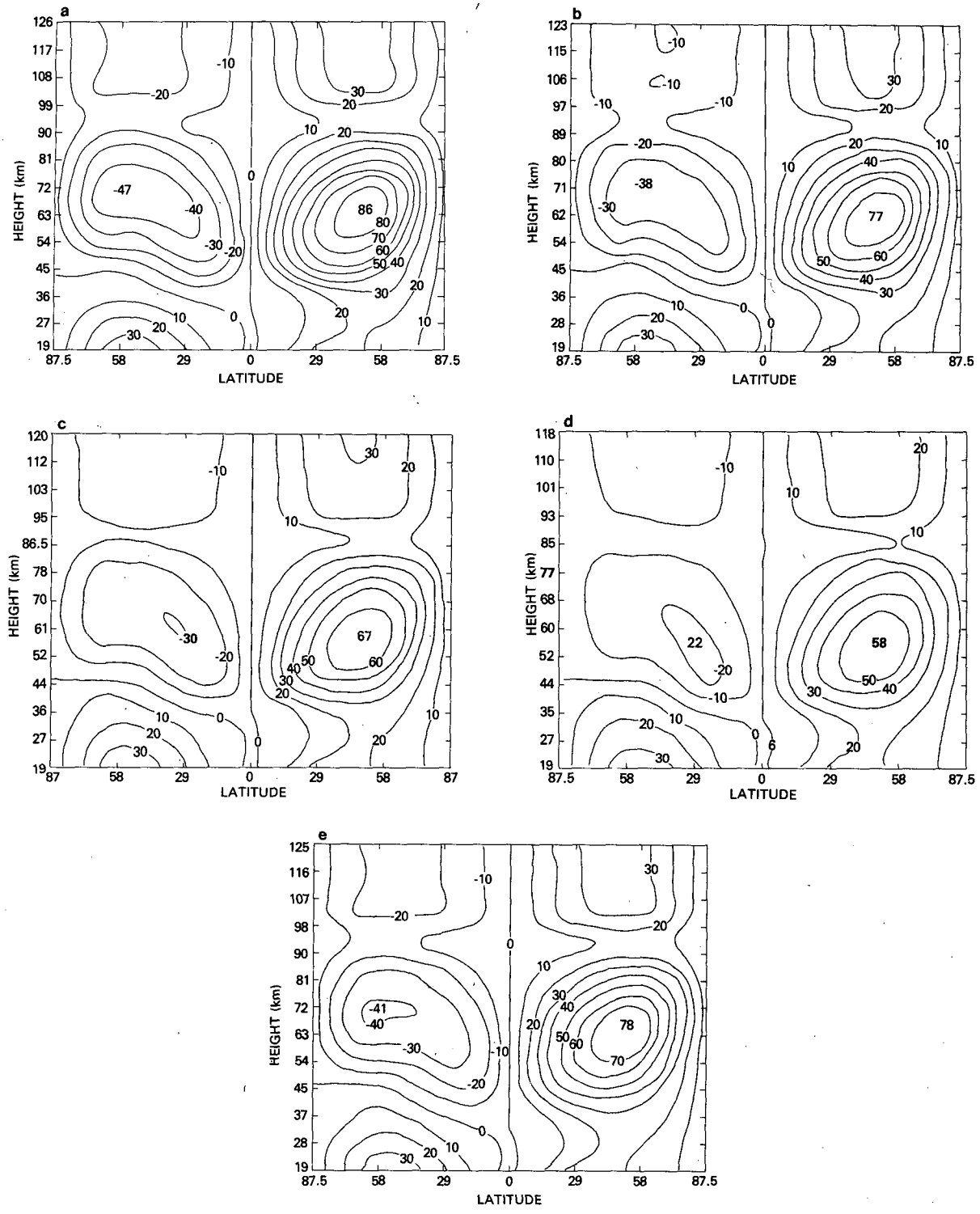

FIG. 3. The steady-state mean zonal wind structure of the upper atmosphere (m s^{-1}). Part (a) is the "normal" structure; parts (b), (c) and (d) show the structure for 25, 50 and 75% reduction in the ozone mixing ratio, respectively; part (e) shows the results for the halocarbon case.

temperature changes of at most 2 K are calculated, which is consistent with the crude estimates of Zerefos and Crutzen (1975). This result is not unexpected in light of the results from the previous section; the O_3 reduction is confined to polar regions and globally the chemical ozone destruction is negligible.

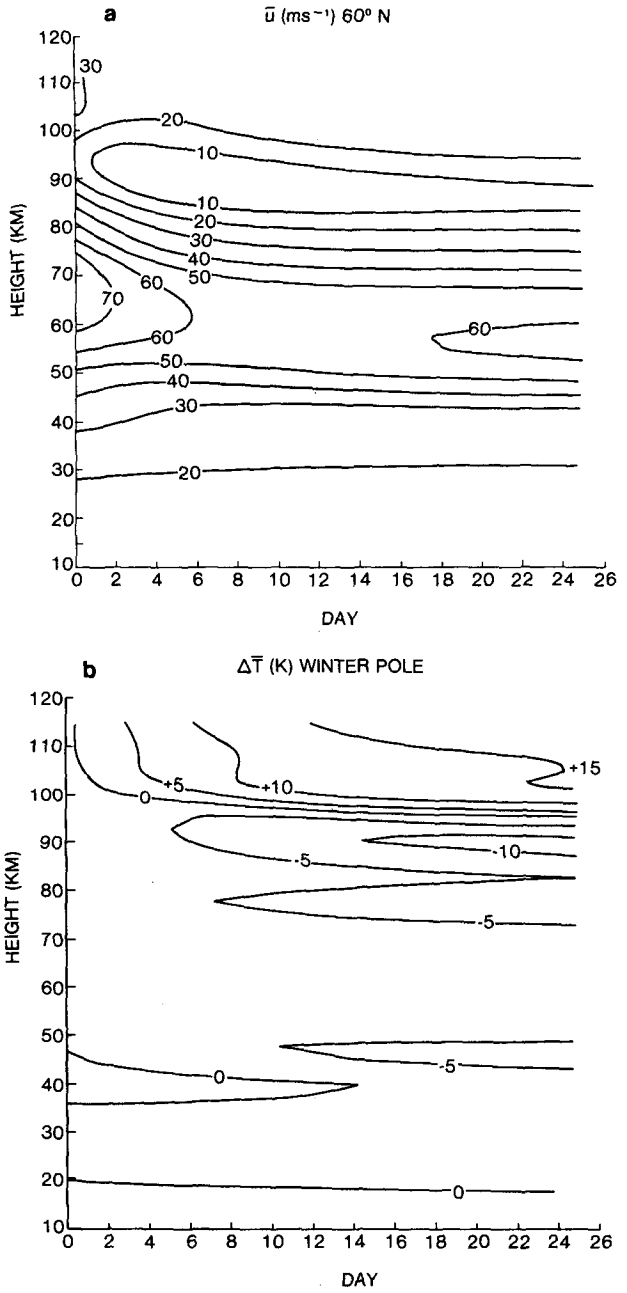

FIG. 4. Time-dependent calculation of the response of the mean circulation to a sudden 75% reduction in O_3: (a) $\bar{u}$ (m s^{-1}), (b) $\bar{T}$ (K).

The second experiment was designed to represent the scenarios predicted by CISC (1976) in their evaluation of halocarbon impact on the ozone layer. The "no chlorine nitrate formation" curve in their Fig. 8.6 was approximated by a suitable linear fit. They predicted a peak global O_3 reduction of 50% at 40 km.

The halocarbon-induced O_3 reduction is projected to occur slowly over decades and a steady-state treatment should suffice. The steady-state results are indicated in Figs. 1–3 by the curves labeled "halocarbon." Substantial changes in the globally averaged heating rate and temperature are evident below 55 km where O_3 reduction becomes significant. The maximum perturbation in $\langle T \rangle$ is 13 K at 43 km. The overall jet structure is similar to the uniform 25% reduction case, but the amplitude change is not as great.

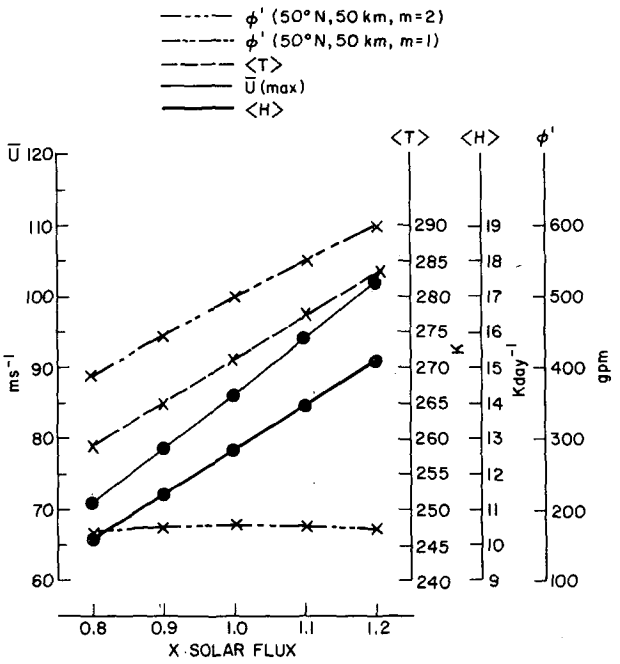

FIG. 5. The response of the stratosphere and mesosphere to solar flux changes. $\langle T \rangle$ is the stratopause temperature, $\langle H \rangle$ the maximum stratospheric heating rate, $\bar{u}$ gives the maximum polar night jet strength, and ϕ' is the geopotential height associated with planetary wavenumbers 1 and 2 at 50 km and 50°N.

Even though the column O_3 density reduction in both cases is 25%, the column O_3 density reduction for the halocarbon case is much less than 25% above 48 km where the peak heating occurs due to the O_3 Hartley lands. This effect produces the major differences between the $\langle H \rangle$ and $\langle T \rangle$ profiles for the 25% reduction and halocarbon experiments. Since the 25% case reaches the same maximum heating rate at a lower altitude, the polar night and day jets have slightly lower intensity because the vertical shear generated from thermal wind relation is sustained over a shorter height interval.

5. Solar flux changes

In the same vein as the uniform ozone density reductions we have examined the model sensitivity to changes in the solar flux. Fig. 5 shows the response of various model variables to altered solar output. This calculation ignores the probably weaker adjustment of O_3 concentrations[1]; however, we believe that is representative of the effects of small variations in solar flux.

It is apparent that the response of the zonally

[1] J. Chang (private communication).

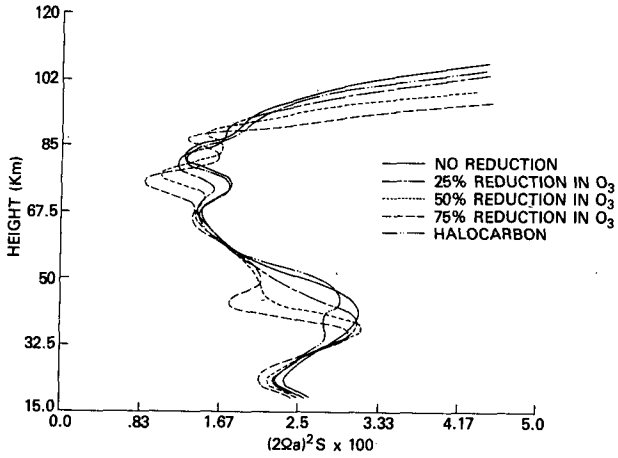

FIG. 6. The static stability $(2\Omega a)^2 S$ as a function of height.

averaged circulation is nearly linear: both the globally averaged stratopause temperature and the strength of the mean zonal winds vary uniformly with flux. At lower altitudes the response is weaker as the tropopause boundary conditions are held fixed for these calculations.

The amplitudes of planetary waves are also shown in Table 1 for the calculated zonal jet structure variation with solar flux. For $m=1$, the amplitude varies nearly linearly with jet strength but its phase is insensitive to jet strength with at most a 7° shift. This is roughly the same magnitude as the phase change between pressure levels of the model. The response of $m=2$ planetary wave is not linear with jet strength and has a maximum amplitude for the 86 m s^{-1} jet (cf. Table 1). Changes in the solar flux on the order of 1% would thus negligibly alter the large-scale wave structure in the upper stratosphere and have an even smaller effect at lower altitudes.

6. Concluding remarks

We have used a numerical quasi-geostrophic model of the mean circulation in the middle atmosphere to investigate the dynamical response to reductions in ozone density. The August 1972 solar proton event produced measurable reductions in the polar O_3 content but minor O_3 destruction on a global basis. Our calculations showed that such an event produces negligible changes in the mean circulation. Halocarbons are predicted to have a global impact on the O_3 layer (CISC, 1976) and we find approximately 10% reduction in the zonal jet strength with smaller percentage changes in the globally averaged temperature. For these realistic O_3 reductions the Dickinson (1973) Newtonian cooling coefficients should adequately represent the IR radiative transfer.

To produce catastrophic effects on the mean circulation we investigated arbitrary uniform O_3 reductions. For 50 and 75% O_3 reductions pronounced changes in the zonal jet structure and globally averaged temperature are obtained. It is unlikely that the results are quantitatively accurate since the IR cooling representation probably breaks down for these large perturbations. We have also ignored explicit eddy transport effects by planetary waves in the middle atmosphere, since they are not yet well understood.

Our results cannot be interpreted as a purely linear response of the atmosphere to a reduction in the differential heating. Changes in the globally averaged thermal structure alter the static stability which is nonlinearly coupled to the vertical velocity. In Fig. 6 we illustrate the effect on the globally averaged static stability for the various ozone reduction cases considered. It should be remembered that the mean circulation has a vertical scale of approximately three scale heights (Leovy, 1964) and will not respond to "small-scale" structure in the static stability. As a consequence the nonlinear coupling is somewhat less than one might infer from Fig. 6.

Hines (1974) suggested that solar-weather interactions may occur by changes in the reflection and transmission properties of the middle atmosphere for planetary waves with solar activity. The August 1972 solar proton event would certainly be an extreme case of solar activity affecting the middle atmosphere. Although local ozone reductions of ~22% occurred in polar regions, the net effect on the mean circulation was negligible. To confirm that the effect on the planetary wave structure was also negligible we performed computations similar to Schoeberl and Geller (1977) for the perturbed and unperturbed atmospheres. The maximum stratospheric change in either amplitude or phase was less than 0.5%. In addition we note that the response time of the mean circulation is probably too long to explain solar-weather coupling, since the response time has the same time scale as the normal transient variation of planetary waves in the lower stratosphere (Hirota and Sato, 1969). A similar calculation was performed for the halocarbon case with resultant change in wave amplitude of about 15% at 50 km for $m=1$ and 10% for $m=2$ at the same altitude. This deviation is still less than the normal winter fluctuations of planetary-wave amplitude. We may conclude from these calculations that the transport and mixing of minor constituents in the stratosphere which occur primarily through planetary-scale eddies will not be substantially altered by predicted O_3 reductions.

Acknowledgments. This research was supported by the Upper Atmosphere Research Office of the National Aeronautics and Space Administration.

REFERENCES

CIRA 1972: *COSPAR International Reference Atmosphere.* Akademie-Verlag, 450 pp.

Committee on Impacts of Stratospheric Change, 1976: *Halocarbons: Effects on Stratospheric Ozone.* Nat. Acad. Sci., 352 pp.

Dickinson, R. E., 1973: Method of parameterization for infrared cooling between altitudes of 30 and 70 kilometers. *J. Geophys. Res.*, **78**, 4451–4457.

Hines, C. O., 1974: A possible mechanism for the production of sun-weather correlations. *J. Atmos. Sci.*, **31**, 589–591.

Leovy, C. B., 1964: Simple models of thermally driven mesospheric circulations. *J. Atmos. Sci.*, **21**, 327–341.

Heath, D., A. J. Krueger and P. J. Crutzen, 1977: Solar proton event: influence on stratospheric ozone. *Science*, **197**, 886–888.

Hirato, I., and Y. Sato, 1969: Periodic variation of the winter stratospheric circulation and intermittent vertical propagation of planetary waves. *J. Meteor. Soc. Japan*, **47**, 390–402.

Schoeberl, M. R., and M. A. Geller, 1977: A calculation of the structure of stationary planetary waves in winter. *J. Atmos. Sci.*, **34**, 1235–1255.

——, and D. F. Strobel, 1978: The zonally averaged circulation of the middle atmosphere, *J. Atmos. Sci.*, **35**, 577–591.

Strobel, D. F., 1976: Parameterization of the atmospheric heating rate from 15 to 120 km due to O_2 and O_3 absorption of solar radiation. NRL Memo. Rep. 3398, Naval Research Laboratory, Washington, D.C. [Available from author, Code 7750, Naval Research Laboratory]. Also *J. Geophys. Res.* (in press) 1978.

Zerefos, C. S., and P. J. Crutzen, 1975: Stratospheric thickness variations over the Northern Hemisphere and their possible relation to solar activity. *J. Geophys. Res.*, **80**, 5041–5043.